J|A|C|S
ARTICLES
Published on Web 10/03/2006

The Conformation of *cyclo*(−D-Pro−Ala$_4$−) as a Model for Cyclic Pentapeptides of the DL$_4$ Type

Markus Heller,[†,‡] Martin Sukopp,[†,⊥] Natia Tsomaia,[§] Michael John,[†,∥] Dale F. Mierke,[§] Bernd Reif,[#] and Horst Kessler*[,†]

Contribution from the Department Chemie, Technische Universität München, Lichtenbergstrasse 4, 85747 Garching, Germany, Department of Molecular Pharmacology, Physiology and Biotechnology, Box B-G4, 171 Meeting Street, Brown University, Providence, Rhode Island 02912, and Forschungsinstitut für Molekulare Pharmakologie, Robert-Rössle-Strasse 10, 13125 Berlin-Buch, Germany

Received May 5, 2006; E-mail: Horst.Kessler@ch.tum.de

Abstract: The conformation of the cyclic pentapeptide *cyclo*(−D-Pro−Ala$_4$−) in solution and in the solid state was reinvestigated using modern NMR techniques. To allow unequivocal characterization of hydrogen bonds, relaxation behavior, and intramolecular distances, differently labeled isotopomers were synthesized. The NMR results, supported by extensive MD simulations, demonstrate unambiguously that the preferred conformation previously described by us, but recently questioned, is indeed correct. The validation of the conformational preferences of this cyclic peptide is important given that this system is a template for several bioactive compounds and for controlled "spatial screening" for the search of bioactive conformations.

Introduction

Rational drug design using natural ligands as templates offers one of the most powerful methodologies for drug discovery, especially in light of recent advances in genome science. In most cases, however, the templates are too large and flexible requiring that they be downsized in order to be used for drug development, while retaining the orientation of the pharmacophoric residues. Cyclic pentapeptides (CPPs)[1] feature a variety of advantages for this task: they are readily synthesized in an automated manner, resistant to proteolysis, and nonimmunogenic. Additionally, CPPs provide enough residues necessary to incorporate the peptide sequence containing the pharmacophore needed for biological activity. Likewise, CPPs are conformationally restricted, enabling the scientist to establish structure−activity relationships using rational spatial screening.[2] This approach was first applied to thymopentin,[3] and then to cyclic RGD peptides, culminating in the αvβ3 selective peptide *cyclo*(−RGDfV−),[4] which was the basis for the development of *Cilengitide* (*cyclo*(−RGDfN(Me)Val−),[5] a peptide in clinical phase II for treatment of gliomas (a brain tumor).[6] A recent example for the importance of CPPs is the molecular-size reduction of a CXCR4 chemokine antagonist using conformation-based-libraries based on cyclic pentapeptides.[7]

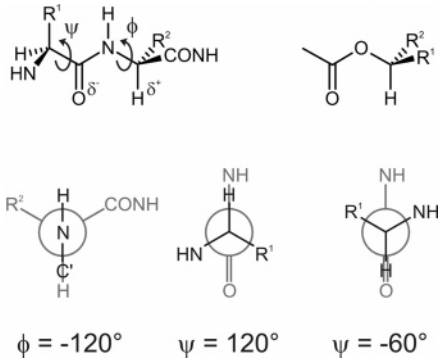

Figure 1. Schematic representation of a peptide backbone illustrating the ϕ and ψ angles (see text). A ϕ angle of −120° is strongly preferred. However, it is important to realize that in many X-ray structures this rule is violated since the conformation in the crystal is fixed by intermolecular hydrogen bonds for most peptides.

The conformational preferences of cyclic peptides can be described using a few general principles. There is a strong tendency for the ϕ dihedral angle to adopt a value of −120°, leading to a parallel orientation of the amide-carbonyl bond vector and the C$^\alpha$H-bond (see Figure 1). This arrangement is

[†] Technische Universität München.
[§] Brown University.
[#] Forschungsinstitut für Molekulare Pharmakologie.
[‡] Present Address: University of British Columbia, Departments of Biochemistry and Molecular Biology, 2350 Health Sciences Mall, Vancouver, BC, V6T 1Z3, Canada.
[⊥] Present Address: BASF Aktiengesellschaft, GVA-B009, 67056 Ludwigshafen, Germany.
[∥] Present Address: Research School of Chemistry, Australian National University, Canberra ACT 0200, Australia.

(1) CPP, cyclic pentapeptide; MAS, magic angle spinning; MD, molecular dynamics; NMR, nuclear magnetic resonance; pA$_4$, *cyclo*(−D-Pro-Ala$_4$−); β-pA$_4$, *cyclo*(−D-Pro−Ala−^{15}N-Ala−Ala−^{13}C′-Ala−); γ-pA$_4$, *cyclo*(−D-Pro−Ala−^{13}C′-Ala−Ala−^{15}N′-Ala−); REDOR, rotational echo double resonance; rmsd, root-mean-square deviation.
(2) Kessler, H.; Gratias, R.; Hessler, G.; Gurrath, M.; Muller, G. *Pure Appl. Chem.* **1996**, *68*, 1201−1205.
(3) Kessler, H.; Kutscher, B.; Klein, A. *Liebigs Ann. Chem.* **1986**, 893−913.
(4) Aumailley, M.; Gurrath, M.; Muller, G.; Calvete, J.; Timpl, R.; Kessler, H. *FEBS Lett.* **1991**, *291*, 50−54.
(5) Dechantsreiter, M. A.; Planker, E.; Matha, B.; Lohof, E.; Holzemann, G.; Jonczyk, A.; Goodman, S. L.; Kessler, H. *J. Med. Chem.* **1999**, *42*, 3033−3040.
(6) Raguse, J. D.; Gath, H. J.; Bier, J.; Riess, H.; Oettle, H. *Oral Oncol.* **2004**, *40*, 228−230.

10.1021/ja063174a CCC: $33.50

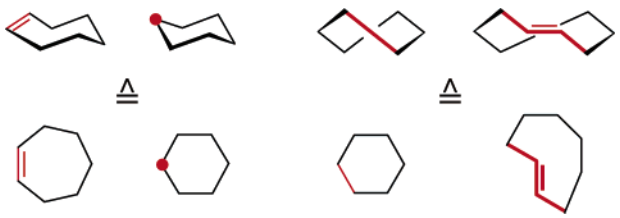

Figure 2. Reduction of cyclic olefins to cycloalkanes. The overall conformational behavior of *cis*-cycloheptene and *trans*-cyclooctene correspond to cyclohexane.

not only sterically preferred but it also orients the dipole charges in optimal directions; a similar preferred orientation is observed in esters. Although this "$\phi = -120°$ rule" is violated in some crystal structures because of strong intermolecular hydrogen bonds, it is valid as a general observation that has been empirically derived from the vast number of peptide structures solved in solution to date.

The ψ angle is less well-defined. A ψ value of $+120°$ (corresponding to a β-strand conformation) or $-60°$ (as observed in α-helices) would be allowed according to a simple analysis of the Ramachandran (ϕ/ψ) map. However, as illustrated in Figure 1, only the $\psi = -60°$ conformation has the flanking amide groups projecting in the same direction in L-amino acids, required for ring closure in a small cyclic peptide. In fact, this is a strongly preferred arrangement, observed in many cyclic peptides. In our experience, the *syn* orientation of the C−O bond with respect to the N−H bond and deviations from $\phi = -120°$ *syn*(C−O/C$^{\alpha}$H) orientation are good metrics for cyclic peptide conformations; the observation of violations of these correlates with structures that have later been shown to be wrong.

One can take the analysis of cyclic peptide conformations a step further by considering that peptide bonds are stereochemically equivalent to double bonds. Hence, a cyclic peptide can be transformed into cyclic hydrocarbons with double bonds. Dunitz and Waser pointed out many decades ago that cyclic olefins can be "converted" into cyclic alkanes by substitution of a *trans*-olefin with a long bond and a *cis*-double bond with a single methylene group.[8] This means that cycloheptene as well as *trans*-cyclooctene correspond to cyclohexane exhibiting a chair and a twist conformation, respectively (see Figure 2).

We have used this principle to explain the conformations of cyclic tripeptides and all-*trans* tetra- and pentapeptides.[2] According to this principle, a cyclic pentapeptide with all-*trans* peptide bonds corresponds to cyclopentane, immediately indicating that high flexibility is expected. The chiralities of the amino acids determine any conformational preference. Hence, the question to be addressed is whether there is a preferred conformation or if there is a rapid equilibrium of more or less equally populated conformations.

NMR evidence was provided that a single D amino acid in the general structure *cyclo*-DL$_4$ exhibits all indicators for a preferred conformation, such as differentiation of amide temperature gradients, H^{N} and H$^{\alpha}$ chemical shifts, and side-chain preference.[9] Hence, we have for a number of years used such cyclic pentapeptides as conformational templates. Our NMR analyses provided evidence for a βII′-turn about the D amino acid ($i + 1$ position) and the following L amino acid ($i + 2$) as well as a γ-turn at the other side of the molecule. Additional NMR studies, however, clearly showed that the γ-turn violates a distance of N*H* to Cα^{i+1}*H*, and agreement could only be obtained by employing ensemble averaging of the NOE restraints over multiple structures involving synchronous rotations about the ϕ and ψ dihedral angles of the residues in the γ-turn.[10]

Recently, the preferred structure of these CPPs, which have proven useful in drug development and for controlled screening for bioactive conformations, was called into question.[11] We therefore undertook a detailed analysis of the parent compound *cyclo*(−D-Pro−Ala$_4$−) (pA$_4$) by (a) synthesis of specifically labeled pA$_4$, (b) measuring scalar couplings across hydrogen bonds to obtain unambiguous evidence of turn structures, (c) analyzing solid-state NMR REDOR data of microcrystalline samples, and (d) long MD trajectories in explicit solvent with and without experimental restraints.

Material and Methods

Synthesis and Purification of Labeled Peptides. Trityl chloride polystyrene resin (PepChem, Tübingen, Germany) was used for peptide syntheses. All fluorenylmethoxycarbonyl- (Fmoc) amino acids and unprotected amino acids were purchased from NovaBiochem (Schwalbach, Germany), Cambridge Isotope Laboratories (Andover, USA) and Martek (Columbia, USA). All reagents and solvents were reagent grade or better and used without further purification. Linear peptides were synthesized by SPPS applying Fmoc strategy.[12,13] Couplings of unlabeled amino acids were performed twice for 1 h at room temperature in *N*-methyl-pyrrolidone (NMP) using a 3-fold excess of *O*-(benzotriazol-1-yl)-*N*,*N*,*N*′,*N*′-tetramethyluronium tetrafluoroborate (TBTU)/*N*-hydroxybenzotriazole (HOBt)/Fmoc-amino acid with 2.8 equiv of DIEA in NMP. Labeled amino acids were coupled with 1.7-fold excess of TBTU/HOBt/Fmoc-amino acid and with 2.8 equiv of DIEA in NMP overnight. The Fmoc-group was removed by sequential treatment of the resins with an excess of 20% piperidine in DMF for 5 and 15 min, respectively. Cleavage of the peptides was achieved by treatment with 20% hexafluoroisopropanol (HFIP) in dichloromethane (DCM) (3 × 10 min) and subsequent evaporation. The linear peptides were cyclizized in solution (concentration 10^{-3} mol/L) with 3 equiv diphenyl phosphoryl azide **(**DPPA) and 5 equiv sodium bicarbonate in *N*,*N*-dimethylformamide (DMF) for 10 h. After filtration and evaporation of the solvent the cyclic peptides were purified by HPLC using a Pharmacia Biotech Series 900 with a reverse phase C-18 column (YMC-Pack ODS/A column) and water and ACN with 0.1% TFA as eluents (gradient: 0−50%; approximately 12.5 min). ESI-MS and RP-HPLC-ESI-MS analyses were performed using a Finnigan LCQ-ESI Spectrometer coupled to a Hewlett-Packard HP1100 HPLC−System.

The following three isotopomers of pA$_4$ were synthesized: pA$_4$ with uniformly ^{15}N,^{13}C-Ala residues, β-pA$_4$ (*cyclo*(−D-Pro−Ala−^{15}N-Ala−Ala−^{13}C′-Ala−)), and γ-pA$_4$ (*cyclo*(−D-Pro−Ala−^{13}C′-Ala−Ala−^{15}N-Ala-)); see also Figure 5 for an illustration.

NMR Spectroscopy. For all liquid-state experiments, a sample containing a 2 mm solution of pA$_4$ peptide in d_6-DMSO (99.5%) was used. Long-range HNCO experiments were recorded at a temperature of 27 °C on a Bruker DMX600 spectrometer equipped with a TXI cryo probe and a single axis gradient system. The long-range HNCO spectra were recorded as 2D versions with the evolution time of the

(7) Fujii, N.; Oishi, S.; Hiramatsu, K.; Araki, T.; Ueda, S.; Tamamura, H.; Otaka, A.; Kusano, S.; Terakubo, S.; Nakashima, H.; Broach, J. A.; Trent, J. O.; Wang, Z. X.; Peiper, S. C. *Angew. Chem., Int. Ed.* **2003**, *42*, 3251−3253.
(8) Dunitz, J. D.; Waser, J. *J. Am. Chem. Soc.* **1972**, *94*, 5645−5650.
(9) Kessler, H. *Angew. Chem., Int. Ed. Engl.* **1982**, *21*, 512−523.
(10) Mierke, D. F.; Kurz, M.; Kessler, H. *J. Am. Chem. Soc.* **1994**, *116*, 1042−1049.
(11) Nikiforovich, G. V.; Kover, K. E.; Zhang, W. J.; Marshall, G. R. *J. Am. Chem. Soc.* **2000**, *122*, 3262−3273.
(12) Carpino, L. A.; Han, G. Y. *J. Org. Chem.* **1972**, *37*, 3404−3409.
(13) Fields, G. B.; Noble, R. L. *Int. J. Pept. Protein Res.* **1990**, *35*, 161−214.

indirect dimension on C′; no solvent suppression was used. All in all, 13 experiments were recorded using the following values for Δ (the dephasing time of the N−C′ coupling): 136, 340, 476, 612, 680, 748, 816, 952, 1020, 1088, 1224, 1292, and 1360 ms. Transverse ^{15}N relaxation rates were measured using a published sequence[14] with a modification of the actual relaxation period, where DIPSI-2 decoupling was applied on the proton channel to mimic the conditions of the long-range HNCO experiment. In total, 14 points were recorded corresponding to relaxation periods of 20 ms and 0.2, 0.4 (2×), 0.6, 0.8, 1.0 (2×), 1.2, 1.4, 1.6 (2×), 1.8, and 2.0 s. The signal intensities were fitted to a monoexponential decay using the Perl-script sparky2rate (http://xbeams.chem.yale.edu/~loria/software.htm).

All solid-state NMR experiments were recorded using ^{1}H,^{13}C cross-polarization with a contact time of 1 ms. ^{13}C 1D experiments were recorded using a recycle delay of 4 s and setting the MAS frequency to 2 kHz. Fitting of the CSA tensor was accomplished using the program SIMPSON.[15] REDOR dephasing and reference experiments[16] were implemented in an interleaved fashion, setting the MAS frequency to 10 kHz, and collecting 640 transients per increment. The dephasing period was incremented in steps of 100 rotor periods yielding a maximum dephasing time of 29 ms. In the REDOR experiments, a recycle delay of 3 s was employed.

The dephasing resonance intensity of a carbon nucleus which is dipolar coupled to a single nitrogen nucleus can be analytically described as[16]

$$S(t) = \int_0^{2\pi} \mathrm{d}\gamma \int_0^{\pi} \mathrm{d}\beta \sin(\beta) \cos(\Phi t) \quad (1)$$

where β and γ represent the Euler angles, and Φ refers to acquired phase because of the N,C dipolar coupling. Φ be expressed as

$$\Phi = \frac{2\pi}{\tau_r}\{\int_0^{\tau_r/2} \mathrm{d}t\, \omega_{NC}^{D}(t) - \int_{\tau_r/2}^{\tau_r} \mathrm{d}t\, \omega_{NC}^{D}(t)\} = b_{NC}\sqrt{2}\sin(2\beta)\sin(\gamma) \quad (2)$$

b_{NC} corresponds to the dipolar coupling constant

$$b_{NC} = \frac{\mu_0 \hbar \gamma_N \gamma_C}{4\pi\, r_{NC}^3}$$

which is related to the distance between the nitrogen and the carbon nucleus. Here, μ_0 represents the permeability of the free space, $\hbar$ corresponds to Planck's constant divided by 2π, and γ_N and γ_C are the gyromagnetic ratios of ^{15}N and ^{13}C, respectively. A reference experiment (S_0) is required to take relaxation effects into account. There, a 180° nitrogen pulse is applied simultaneously with the ^{13}C 180° refocusing pulse in the middle of the pulse sequence which refocuses the N,C dipolar coupling. N−C′ distances were obtained by fitting the experimental REDOR dephasing curves to the equation ($S_0 - S/S_0$).

Molecular Dynamics Simulations. An initial structure of the cyclic peptide pA$_4$ was constructed with dihedral angles characteristic to βII′ and γ turns. The structure was energy minimized in vacuo with conjugate gradients using the AMBER force field, ignoring charges. The DISCOVER (Molecular Simulations, Inc.) program within the molecular modeling package Insight II was used for minimization. Molecular dynamics simulations were performed with the GROMACS 3.2.1 software package.[17] To model an explicit solvent environment, the peptide structure was placed in the simulation box ($x = y = z =$ 40 Å) containing typically 487 DMSO molecules. All atoms were treated in the OPLS-AA (optimized potentials for liquid simulations—all-atom) force field. The complete system was energy-minimized using a steepest descent algorithm. The experimental distances derived from REDOR were then introduced as constraints (force constant 500 KJ mol^{-1} nm^{-1}) and the MD simulation at 300 K (with 0.02 ps temperature bath coupling) was performed for 2 ns. The velocities were recorded, the constraints were removed, and the MD simulation was continued for 38 ns without any restraints. During the simulation the integration time step was 1 fs, and the applied constant pressure was 1 bar. All simulations were performed on Pentium III processors running Linux.

Results

High-Resolution NMR. Long-range HNCO experiments were performed with a pA$_4$-sample with uniformly ^{13}C,^{15}N-labeled alanines dissolved in d_6-DMSO. In panel A of Figure 3, a spectrum recorded with the evolution time for the N−C′ coupling, Δ, set to $7/(2^1J_{NC'}) = 238$ ms is shown. All three expected direct correlations are observed; in addition, a weak peak corresponding to an intraresidual correlation Ala2H^N−Ala2C′ is found. For the spectrum depicted on panel B, Δ was set to $4/^1J_{NC'} = 272$ ms in order to suppress the direct one-bond couplings. The box indicates the position where a cross-peak corresponding to the hydrogen bond in the γ-turn is expected. Note that the chemical shifts of Ala2C′ and Ala5C′, the hydrogen bond acceptor in the βII′-turn, differ only by 0.03 ppm (see Table 1); thus, it is difficult to tell whether the observed peak corresponds to a residual one-bond correlation or to a correlation via the hydrogen bond. A signal indicating the γ-turn is not observed at all.

Up to this point, the HNCO spectrum shown in panel B yields no information about hydrogen bonds. As reported earlier, Mierke and co-workers found a stable βII′-conformation with D-Pro1 in the $i + 1$ position for pA$_4$;[10] thus, at least one cross-peak corresponding to the hydrogen bond Ala3H^N···Ala5C′ would be expected. Unfortunately, this peak cannot be unambiguously identified because of severe signal overlap with Ala3H^N−Ala2C′. In contrast, while the position of the cross-peak of the γ-turn is not affected from spectral overlap, only one of the five conformers found for pA$_4$ possesses the γ-turn.[10]

In principle, there are two major reasons why hydrogen bonds might be hard to probe using pA$_4$ with uniformly ^{15}N and ^{13}C labeled Ala-residues: resonance overlap and fast transverse relaxation of the ^{15}N nuclei, both of which have been overcome by selective labeling.

Figure 4 shows plots of the transfer amplitude A of the HNCO experiment (eq 3) assuming $^{3h}J_{NC'} = 0.3$ Hz and neglecting all passive couplings J':[18,19]

$$A \propto \exp(-2\Delta R_{2,\mathrm{app}}) \sin^2(\pi\, {}^{3h}J_{NC'}\Delta) \prod \cos^2(\pi J'\Delta) \quad (3)$$

The curves were calculated without relaxation (solid line), and assuming apparent transverse relaxation rates of 1 s^{-1} (long dashes) and 5 s^{-1} (short dashes). These plots immediately suggest that couplings on the order of 0.3 Hz or smaller are difficult to detect if a wide range of Δ is to be sampled and transverse relaxation becomes significant.

To overcome both issues, two isotopomers have been synthesized in which only the hydrogen donor and acceptor positions of the βII′- and γ-turn were isotopically labeled. These

(14) Farrow, N. A.; Muhandiram, R.; Singer, A. U.; Pascal, S. M.; Kay, C. M.; Gish, G.; Shoelson, S. E.; Pawson, T.; Formankay, J. D.; Kay, L. E. *Biochemistry* **1994**, *33*, 5984−6003.
(15) Bak, M.; Rasmussen, J. T.; Nielsen, N. C. *J. Magn. Reson.* **2000**, *147*, 296−330.
(16) Gullion, T.; Schaefer, J. *J. Magn. Reson.* **1989**, *81*, 196−200.
(17) Berendsen, H. J. C.; Vanderspoel, D.; Vandrunen, R. *Comput. Phys. Commun.* **1995**, *91*, 43−56.
(18) Cordier, F.; Grzesiek, S. *J. Am. Chem. Soc.* **1999**, *121*, 1601−1602.
(19) Cornilescu, G.; Hu, J. S.; Bax, A. *J. Am. Chem. Soc.* **1999**, *121*, 2949−2950.

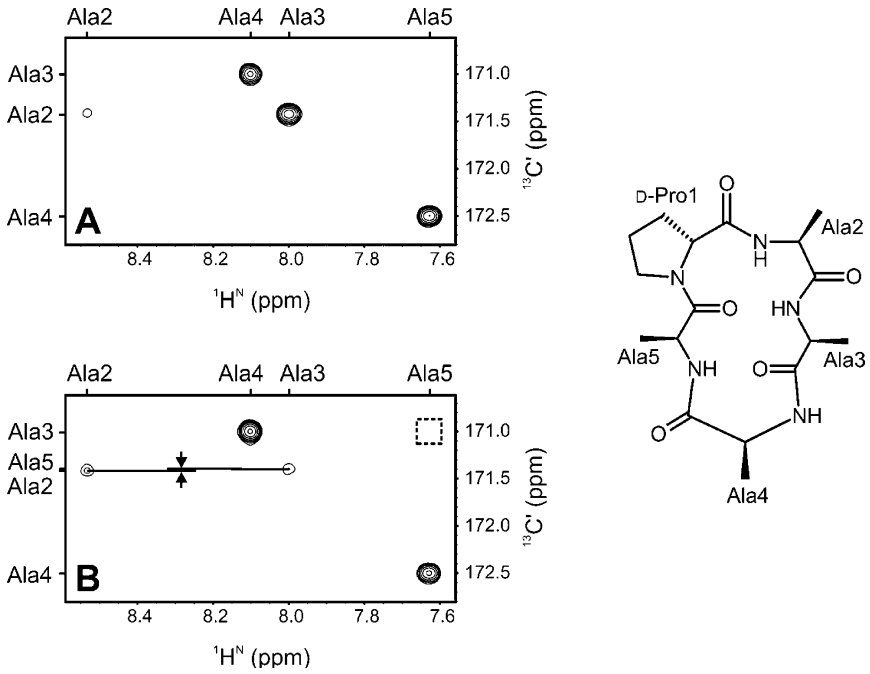

Figure 3. Long-range HNCO spectra of pA4. In panel A, the evolution time for the N−C′ coupling, Δ, was set to $7/(2^1J_{NC'}) = 238$ ms, and the three direct one-bond correlations as well as a weak two-bond intraresidual correlation (Ala2H^N−Ala2C′) are observed. In panel B, Δ = 272 ms. A cross-peak is observed for the βII′-turn (Ala3H^N−A5C′); a correlation corresponding to the γ-turn (expected position indicated by the box) is not observed. Note that the chemical shifts of Ala2C′ and Ala5C′ (indicated by the horizontal lines) differ by only 0.03 ppm.

Table 1. H^N, N, and C′ Shifts of *cyclo*(−D-Pro−Ala4−)[a]

	δ(H^N)	δ(N)	δ(C′)[b]
Ala2	8.5	124.9	171.42
Ala3	8.0	121.7	171.00
Ala4	8.1	122.8	172.50
Ala5	7.6	113.3	171.39

[a] All chemical shifts are given in parts per million (ppm). Note that D−Pro1 was not isotopically labeled, hence, no chemical shift data is available for this residue. [b] Chemical shifts for C′ are given with a precision of 2 digits to allow for a distinction between Ala2C′ and Ala5C′.

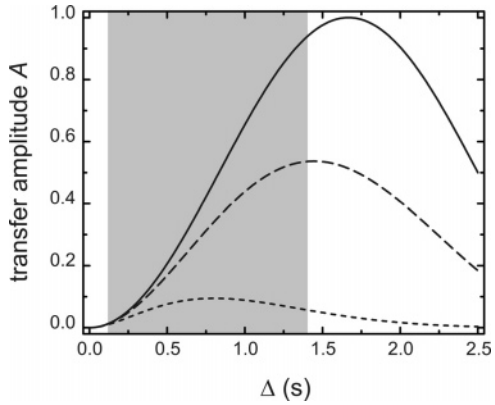

Figure 4. Plots of transfer amplitudes of the long-range HNCO experiment (eq 3). The curves were calculated without relaxation (solid line), and assuming apparent transverse relaxation rates of 1 s^{-1} (long dashes) and 5 s^{-1} (short dashes). $^{3h}J_{NC'}$ was assumed to be 0.3 Hz, and all passive couplings were neglected. The shaded area indicates the range of values for Δ that was sampled in the HNCO experiments.

compounds will be referred to as β-pA4 (*cyclo*(−D-Pro−Ala−^{15}N-Ala−Ala−^{13}C′-Ala−)), where the donor and acceptor positions of the βII′-turn were labeled, and γ-pA4 for its γ-turn counterpart (*cyclo*(−D-Pro−Ala−^{13}C′-Ala−Ala−^{15}N-Ala−)) (see Figure 5 for an illustration).

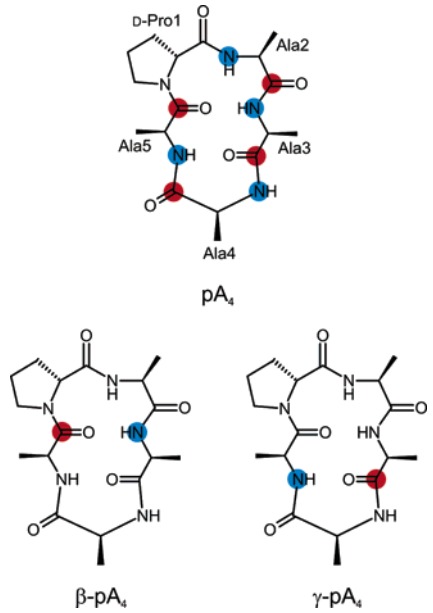

Figure 5. Illustrations of the different pA4 isotopomers used in this study. Red and blue circles indicate ^{13}C and ^{15}N labels, respectively. These compounds are referred to as pA4 (*cyclo*(−D-Pro−Ala4−) with uniformly ^{13}C,^{15}N-labeled Ala residues), β-pA4 (*cyclo*(−D-Pro−Ala−^{15}N-Ala−Ala−^{13}C′-Ala−)), and γ-pA4 (*cyclo*(−D-Pro−Ala−^{13}C′-Ala−Ala−^{15}N-Ala-)).

At first, the effect of the selective labeling scheme on transverse relaxation rates was investigated. As expected, ^{1}H,^{15}N-HSQC experiments of both β-pA4 and γ-pA4 contained only one signal. Estimations of ^{15}N $R_{2,app}$ in uniformly and selectively labeled pA4 showed that transverse relaxation is slower by a factor of ∼5 in the selectively labeled peptides (measured $R_{2,app}$ are given in Table 2), suggesting improved sensitivity for the long-range HNCO experiments (see Figure 4).

Table 2. Apparent Transverse ^{15}N Relaxation Rates $R_{2,app}$ for Uniformly and Selectively Labeled pA_4

	Ala3N		Ala5N		Ala2N
sample	pA_4	β-pA_4	pA_4	γ-pA_4	pA_4
$R_{2,app}$ (s^{-1})	4.75 ± 0.08	0.96 ± 0.01	4.88 ± 0.12	0.93 ± 0.01	2.94 ± 0.14

Consequently, HNCO experiments were repeated for β- and γ-pA_4. In HNCO experiments with Δ set to $1/(2^1J_{NC'})$, only a weak signal arising from the natural abundance ^{13}C nuclei directly bound to a ^{15}N amide was observed (not shown). This signal was readily suppressed in long-range HNCO experiments by adjusting $\Delta = 1/(^1J_{NC'})$ individually for both peptides. Values for Δ were 68 ms for β-pA_4 and 72 ms for γ-pA_4, corresponding to $^1J_{NC'}$ of 14.7 Hz (Ala3*N*−Ala2*C*′) and 13.9 Hz (Ala5*N*−Ala4*C*′), respectively; $^1J_{NC'}$ for Ala4*N*−Ala3*C*′ was estimated to be 13.5 Hz. Representative long-range HNCO spectra of β-pA_4 and γ-pA_4 are shown in Figure 6.

Juranic et al. have reported the largest $^1J_{NC'}$ coupling constant in reverse β-turns for the amide nitrogen of the residue in the $i + 3$ position (in our case β-pA_4),[20] while the weakest coupling was found for the residue in the $i + 2$ position. Indeed, the largest $^1J_{NC'}$ in pA_4 is observed for Ala3*N*−Ala2*C*′. Ala2*N*−Pro*C*′ in the $i + 2$ position does not yield a signal in the HNCO experiments, since D-Pro1 is not isotopically labeled. Thus, the existence of the βII′-turn is already corroborated by the one-bond couplings.

Subsequently, for the measurement of the coupling constants, a series of long-range HNCO experiments were recorded for each selectively labeled peptide, with values for Δ ranging from roughly 140 ms to 1.4 s, corresponding to $20/(^1J_{NC'})$. The experimental data including best fits to eq 3 are shown in Figure 7. Fitting was performed neglecting all passive couplings since both molecules are selectively labeled. As such, any passive couplings should be marginal if not absent. Values for apparent transverse relaxation rates are given in Table 2. The resulting $^{3h}J_{NC'}$ of 0.31 ± 0.01 Hz obtained for β-pA_4 and 0.38 ± 0.02 Hz for γ-pA_4 are in good agreement with values reported in the literature (see discussion).

Given that the long-range HNCO experiments for both peptides were recorded under identical conditions and that all spectra were processed identically, the populations of conformations featuring a β- and a γ-turn can be roughly estimated using the cross-peak signal intensities under the following assumptions: (i) identical concentrations of both samples, (ii) identical coupling constants $^{3h}J_{NC'}$, and (iii) identical line widths of the cross-peaks in both dimensions. Identical concentrations can be assumed within the error introduced by weighing out the peptides, and the coupling constants obtained are very similar. While both cross-peaks have similar line widths in the proton dimension (18 Hz for β-pA_4 and 22 Hz for γ-pA_4), the carbonyl carbon line widths differ by 10 Hz (27 Hz for β-pA_4 and 37 Hz for γ-pA_4). Approximating the peaks as cones with an elliptical base, it is easily envisioned that a difference of 10 Hz in line width translates into a ratio of peak heights of less than 2. The ratio of peak heights observed for our experimental data is, however, close to 10. Hence it can be concluded that the population of conformations featuring a γ-turn is in the range of 15−30%. It is worth noting that larger line widths and thus larger apparent transverse relaxation rates are observed for γ-pA_4, since this observation might be explained by a chemical exchange contribution to transverse relaxation.

Solid-State NMR. To delineate the hydrogen bonding characteristics of the cyclic pentapeptides in a complementary way, we carried out MAS solid-state NMR experiments using selectively labeled peptides to measure heteronuclear N−C′ distances in REDOR experiments.[16] The experiments were recorded at a magic angle spinning (MAS) frequency of 10 kHz for β-pA_4 and γ-pA_4; the experimental results are shown in Figure 8.

The best fit with the lowest rmsd value between experimental and simulated data was obtained for dipolar couplings corresponding to distances of 4.03 ± 0.06 and 3.39 ± 0.03 Å for Ala3N−Ala5C′ (β-pA_4) and Ala3C′−Ala5N (γ-pA_4), respectively.

Table 3 lists the average distances between Ala3N−Ala5C′ and Ala3C′−Ala5N obtained from REDOR experiments and two sets of conformers obtained from a MD trajectory (see later for details). The distances derived from the REDOR experiments are in excellent agreement with the MD results; all deviations are within the errors of the REDOR distances. Remarkably, the REDOR distances are virtually identical to those in conformers II and IV (see Figure 11).

In addition to the N−C′ distances, the H^N−N distances have been measured for Ala3 and Ala5. It seems intuitive that these distances can be significantly elongated if the atoms are involved in a strong hydrogen bond. This phenomenon has been reported for the $N^{\delta1}$−H moiety of His·HCl·H_2O, where an elongation of 4 pm has been attributed to a strong hydrogen bond between the $N^{\delta1}$ proton and the carboxy-group of a molecule in a neighboring unit cell.[21] In pA_4, however, the H^N−N distances in Ala3 and Ala5 are identical within error (data not shown).

Furthermore, we measured the carbonyl CSA tensor which directly reflects the chemical environment of a nuclear spin and which is indicative for hydrogen bonding. Figure 9 shows experimental and simulated 1D ^{13}C spectra of β-pA_4 and γ-pA_4 acquired at a MAS frequency of 2 kHz. Obviously, the shape of the spinning sideband pattern differs for Ala5C′ (panel A) and Ala3C′ (panel B), indicating a different asymmetry parameter η of the $^{13}C'$ CSA tensors.

Table 4 represents the CSA parameters obtained for β- and γ-pA_4, as well as values for the crystalline tripeptide Ala−Gly−Gly obtained by Tycko et al., which are included in the table for reference.[22] The individual components of the CSA tensor, δ_{11}, δ_{22}, and δ_{33}, are similar for both pA_4 samples, yielding an identical isotropic chemical shift. While δ_{11} and δ_{22} are in good agreement with the values reported by Tycko and co-workers, δ_{33} is at variance. The magnitude of the CSA, $\Delta\delta$, is in good agreement for β- and γ-pA_4, but is roughly 20 ppm smaller than $\Delta\delta$ as obtained in the literature. The asymmetry parameter η for β-pA_4 is identical to the reported value, but the fit for γ-pA_4 yielded $\eta = 1$. The observation that the anisotropy $\Delta\delta$ is decreased compared to reference values indicates a scaling of the anisotropic interaction owing to molecular dynamics in the static case. The fact that the asymmetry of Ala3C′ is equal

(20) Juranic, N.; Ilich, P. K.; Macura, S. *J. Am. Chem. Soc.* **1995**, *117*, 405−410.
(21) Zhao, X.; Sudmeier, J. L.; Bachovchin, W. W.; Levitt, M. H. *J. Am. Chem. Soc.* **2001**, *123*, 11097−11098.
(22) Tycko, R.; Weliky, D. P.; Berger, A. E. *J. Chem. Phys.* **1996**, *105*, 7915−7930.

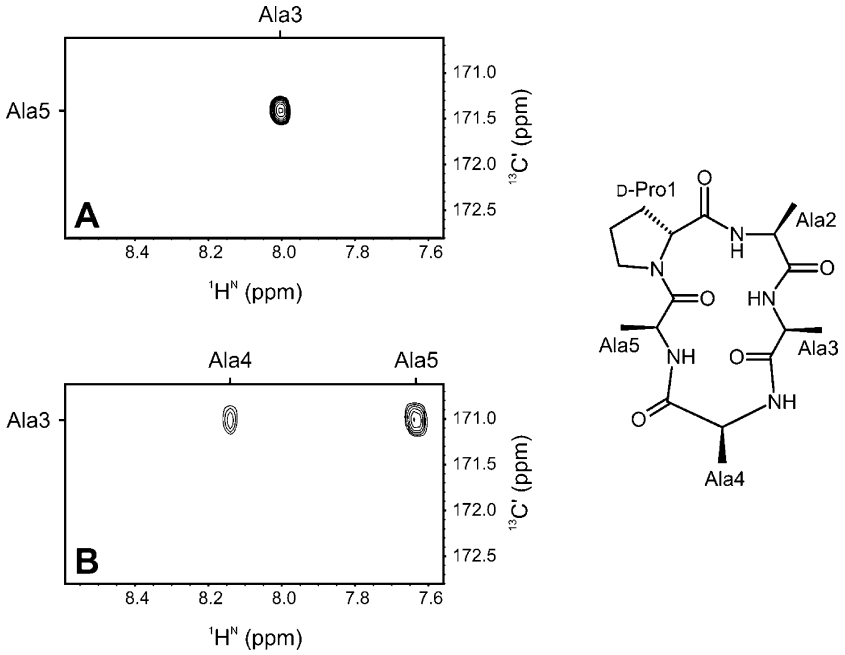

Figure 6. Long-range HNCO spectra of β-pA$_4$ (panel A) and γ-pA$_4$ (panel B) recorded with Δ set to $12/(^1J_{NC'})$, corresponding to 816 ms for β-pA$_4$ and 864 ms for γ-pA$_4$. The peak corresponding to the correlation Ala4H^N−Ala3C′ can be attributed to insufficient washing during the synthesis of γ-pA$_4$.

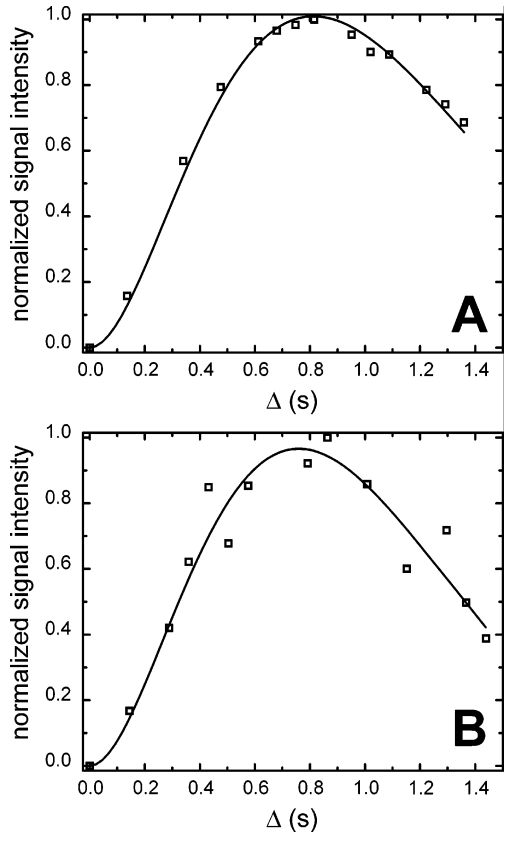

Figure 7. Plots of the long-range HNCO signal intensities versus the dephasing time Δ for β-pA$_4$ (Ala3H^N−Ala5C′, panel A) and γ-pA$_4$ (Ala3C′-Ala5H^N, panel B). The solid lines represent the best fits using eq 3 neglecting all passive couplings. Fitted $^{3h}J_{NC'}$ are 0.31 ± 0.01 Hz for β-pA$_4$ and 0.38 ± 0.02 Hz for γ-pA$_4$.

to 1 indicates a chemical exchange process.[23] Measurements of dynamic effects were recently reported for several uniformly labeled, microcrystalline peptides and proteins.[24−26] In addition, deuterium MAS solid-state NMR experiments on perdeuterated

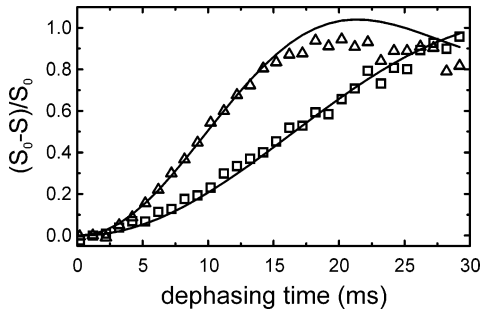

Figure 8. REDOR dephasing curves ($(S_0 - S)/S_0$) for β-pA$_4$ (squares) and γ-pA$_4$ (triangles). The symbols represent the experimental data, while the solid lines correspond to the best fit. N−C′ distances obtained from the fits were 4.03 ± 0.06 Å for β-pA$_4$ and 3.39 ± 0.03 Å for γ-pA$_4$.

Table 3. Comparison of Averaged N−C′ Distances (in Å) for Different pA$_4$ Structures

structure	*d* (Ala3N–Ala5C′) (Å)	*d* (Ala3C′-Ala5N) (Å)
REDOR[a]	4.03	3.39
<I>[b]	4.07	3.18
<II>[c]	4.04	3.39

[a] Results from the REDOR experiment; errors were estimated to be less than ± 5%. [b] Average distance for conformation I from a 40 ns MD trajectory (see Figure 11). [c] Average distance for conformation II from a 40 ns MD trajectory (see Figure 11).

proteins provided detailed motional models for uniformly isotopically enriched proteins.[27,28]

Recently, Sattler and co-workers found that the downfield component δ_{11} and the central component δ_{22} of the carbonyl

(23) Mehring, M. *Principles of High Resolution NMR in Solids*, 2nd ed.; Springer-Verlag: Berlin, 1983.
(24) Giraud, N.; Bockmann, A.; Lesage, A.; Penin, F.; Blackledge, M.; Emsley, L. *J. Am. Chem. Soc.* **2004**, *126*, 11422−11423.
(25) Seidel, K.; Etzkorn, M.; Sonnenberg, L.; Griesinger, C.; Sebald, A.; Baldus, M. *J. Phys. Chem. A* **2005**, *109*, 2436−2442.
(26) Giraud, N.; Blackledge, M.; Goldman, M.; Bockmann, A.; Lesage, A.; Penin, F.; Emsley, L. *J. Am. Chem. Soc.* **2005**, *127*, 18190−18201.
(27) Hologne, M.; Faelber, K.; Diehl, A.; Reif, B. *J. Am. Chem. Soc.* **2005**, *127*, 11208−11209.
(28) Hologne, M.; Chen, Z.; Reif, B. *J. Magn. Reson.* **2006**, *179*, 20−28.

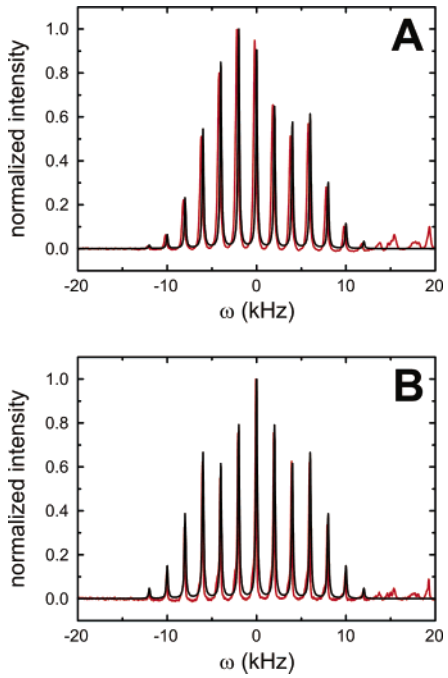

Figure 9. Experimental (red) and simulated (black) 1D ^{13}C spectra of β-pA$_4$ (panel A) and γ-pA$_4$ (panel B) acquired at a MAS frequency of 2 kHz. The experiments were recorded at an external magnetic field of 11.7 T, corresponding to a ^1H Larmor frequency of 500 MHz.

Table 4. Components of the Carbonyl C′ CSA Tensor for β-pA$_4$ and γ-pA$_4$ Obtained by Fitting 1D ^{13}C Spectra Recorded at a MAS Frequency of 2 kHz[a]

	δ_{iso}[b]	$\Delta\delta$[c]	η[d]	δ_{11}[e]	δ_{22}[e]	δ_{33}[e]
β-pA$_4$ (Ala5C′)	171.3	77.1	0.76	230	172	133
γ-pA$_4$ (Ala3C′)	171.0	80.3	1	232	178	125
Tycko et al.	171.0	106.5	0.76	242	182	89

[a] As a comparison, values reported by Tycko and co-workers are given.[22] [b] Isotropic chemical shift (ppm). [c] Chemical shift anisotropy. [d] Asymmetry parameter. [e] Components of the CSA tensor (ppm).

CSA tensor are decreasing and increasing, respectively, upon hydrogen bonding.[29] At the same time, the upfield component δ_{33} remains virtually unchanged. We do not observe this trend in our solid-state NMR experiments. Instead, we find a reduced CSA tensor (see Table 4) compared to previous investigations.[22] In addition, we observe an unexpectedly large asymmetry for γ-pA$_4$ ($\eta = 1$). Conformational averaging in the solid-state indeed yields a decrease of the CSA tensor in concert with an increased asymmetry;[30] hence, our carbonyl CSA data support the conformational flexibility observed in the MD calculations for residues involving amino acids Ala3 and Ala4 in pA$_4$. On the other hand, our data rule out the presence of a strong hydrogen bond (see below).

Molecular Dynamics. To examine the energetic stability of the βII′γ structure as deemed by a molecular mechanics program, a molecular dynamics simulation on pA$_4$ was performed in explicit DMSO solvent for 40 ns using the OPLS force field. During the initial 2.1 ns, the two REDOR-derived distances (Ala3N−Ala5C′ and Ala3C′−Ala3N) were applied to allow the system to come to equilibrium; for the remainder of the trajectory, 37.9 ns, the system was allowed to evolve

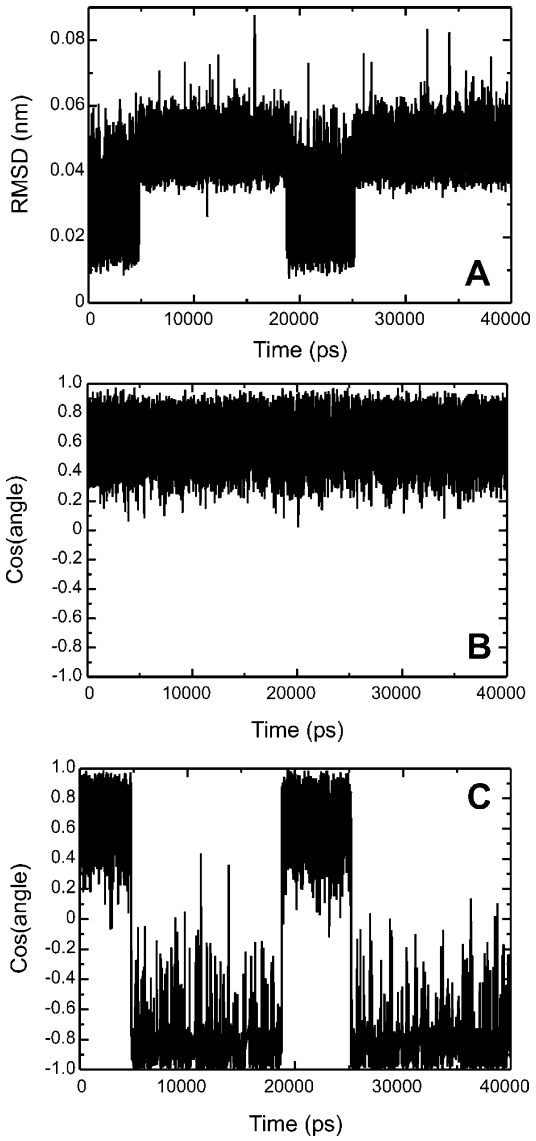

Figure 10. (A) A rmsd plot of the peptide backbone after a least-squares fit to the initial backbone structure. (B) Cosine of the angle between the C−O vector of Ala5 and the peptide ring plane defined by three atoms, Ala2Cα, Ala3Cα, and Ala5C′. The angle fluctuates, but remains in the same range during the entire 40 ns MD simulation. **(C)** Cosine of the angle between the C−O vector of Ala3 and the peptide ring plane defined by three atoms, Ala5Cα, Ala2Cα, and Ala3C′. The angle changes periodically as the amide bond Ala3C′−Ala4N rotates in the γ-turn region of the peptide, as illustrated by the stereoplots depicted in Figure 11.

freely. On the basis of the rmsd of the peptide backbone (see Figure 10A), there are conformational transitions at 5, 18, and 25 ns of the simulation, with representative structures illustrated as stereoplots in Figure 11. The conformational transition is the rotation of the Ala3−Ala4 peptide plane, induced by a ∼180° rotation of the ψ-Ala3/ϕ-Ala4 pair of dihedral angles. This behavior is reflected in the variations of the C′ vectors of Ala3 and Ala5 with respect to the peptide ring plane. Representations of the trajectory of the angle between the C′ vectors and a plane representing the molecular coordinate system, defined by the two Cα carbons and the C′ of the investigated H-bond, show that the angle remains within a narrow range for the Ala5C′ vector (Figure 10B), whereas it flips for Ala3C′ (Figure 10C). The MD simulations show that the βII′-turn region is stable throughout the entire simulation.

(29) Markwick, P. R. L.; Sattler, M. *J. Am. Chem. Soc.* **2004**, *126*, 11424−11425.
(30) Schmidt-Rohr, K.; Spiess, H. W. *Multidimensional Solid-State NMR and Polymers*; Academic Press: London, 1994.

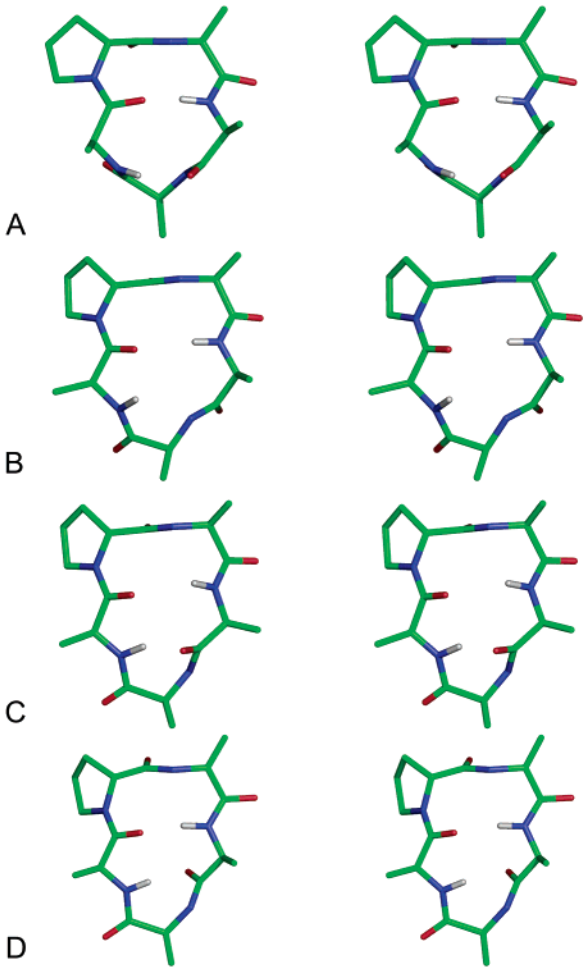

Figure 11. Representative structures observed during the MD simulation:. (A) 0 ns to 5 ns, (B) 5 ns to 18 ns, (C) 18 ns to 25 ns, (D) 25 ns to 40 ns. The peptide backbones are color-coded (red = oxygen, green = carbon, blue = nitrogen, white = hydrogen). Only two amid hydrogens (Ala3H^N and Ala5H^N) are displayed for clarity. The βII′-turn remains undisturbed throughout the 40 ns long simulation maintaining the hydrogen bond between Ala3H^N and Ala5C′. In the γ-turn region, however, the amide plane between Ala3−Ala4 undergoes transitions induced by a 180° rotation about the ψ-Ala3 and ϕ-Ala4 pair.

In addition, a MD simulation was performed using the same conditions and employing the 20 NOE distances as reported by Mierke et al. as initial restraints.[10] The results of this run are essentially the same as described in the above paragraph and are therefore not discussed further.

All of the structures depicted in Figure 11 feature a hydrogen bond Ala3H^N···Ala5C′ as part of a βII′-turn, as indicated by the backbone dihedrals ϕ and φ (see Supporting Information for a table of all ϕ and ψ angles). For D-Pro1, the average values are $\phi = 67.6°$ (60°) and $\varphi = -116.6°$ (120°); for Ala2, $\phi = -93.8°$ (−80°) and $\varphi = 5.7°$ (0) were observed (values in parentheses are the values for an idealized βII′-turn); the average distance between Ala3N and Ala5O is 3.2 Å. In contrast, the carbonyl group of Ala3 points to the same side as the amide moiety of Ala5 in conformation I (observed between 0 and 5 ns and 18−25 ns), while the amide protons of Ala4 and Ala5 are on the same side in conformation II (observed 5−18 ns, and 25−40 ns). This behavior suggests that a γ-turn is present in conformation I, as corroborated by the average values of ϕ and ψ of $\phi = 79.1°$ (75°) and $\psi = -48.4°$ (−64°).

Discussion

Hydrogen bonds have long been important parameters in the determination of protein structures. While $^{3h}J_{NC'}$ have been measured for a large number of proteins, detailed data including residues located in turn structures were published only for four proteins: ubiquitin,[18,19,31,32] an immunoglobulin binding domain of streptococcal protein G,[33] the cold shock protein A from *E. coli*,[34] and the superoxide dismutase[35] but not for small cyclic peptides. In all of these studies, $^{3h}J_{NC'}$ values were primarily obtained for hydrogen bonds between residues located in elements of secondary structure. While the observed coupling constants (absolute values, since $^{3h}J_{NC'} < 0$) in β-sheets are larger than in α-helices (for ubiquitin, the average coupling constants are 0.65 ± 0.14 Hz for β-sheets and 0.38 ± 0.12 Hz for α-helices),[18] they are smaller for residues located in turns. With one exception for ubiquitin, absolute values of $^{3h}J_{NC'}$ are smaller than 0.3 Hz for five residues involved in turns (three type I, two type II; data taken from refs 18, 19, 34). For the cyclic peptide used in this study, coupling constants of 0.31 ± 0.01 Hz for the βII′-turn and 0.38 ± 0.02 Hz for the γ-turn have been determined using long-range HNCO experiments; these values are in good agreement with values reported in the references given above.

The strength of hydrogen bonds correlates with the magnitude of the coupling constants. It is well-known that intramolecular hydrogen bonds in cyclic penta- and hexapeptides are relatively weak,[36] as indicated by the upfield shift of the amide protons in intramolecular hydrogen bonds as opposed to the downfield shift of amide protons which are solvated by the strong binder DMSO.[9] The conformation of cyclic peptides is most strongly determined by the stereochemistry of the substitution. For example, *N*-methylation of the hydrogen bond donor, i.e., the amide in the $i + 3$ position of a βII′ turn in a LDLL sequence, does usually not alter the ϕ/ψ angles about residues in positions $i + 1$ and $i + 2$, which are usually used to define the β turn, although the NMe group prevents the formation of the hydrogen bond.

On the basis of the 40 ns MD simulations, greatly exceeding the previous trajectories of Mierke et al. of 20 ps,[10] the conformation including a βII′-turn with D-Pro1 in the $i + 1$ position is seen to be energetically stable, with averaged backbone dihedral angles which are close to the ideal values for such a turn. On the other hand, the carbonyl bond vector of Ala3 rotates periodically in the γ-turn region, suggesting a dynamic behavior for this part of the molecule. This behavior is indeed supported by the CSA data obtained from solid-state NMR experiments, namely a reduced chemical shift anisotropy in concert with an increase in asymmetry for Ala3C′. In addition, the N−C′ distances of the hydrogen bond donors and acceptors were determined for microcrystalline samples of β- and γ-pA$_4$. The distances obtained from REDOR experiments are in excellent agreement with the distances of conformer II, suggesting that the γ-turn (conformation I, Figure 11) is only slightly populated in the solid state. This is in accordance with

(31) Cordier, F.; Grzesiek, S. *J. Mol. Biol.* **2002**, *317*, 739−752.
(32) Cordier, F.; Grzesiek, S. *Biochemistry* **2004**, *43*, 11295−11301.
(33) Cornilescu, G.; Ramirez, B. E.; Frank, M. K.; Clore, G. M.; Gronenborn, A. M.; Bax, A. *J. Am. Chem. Soc.* **1999**, *121*, 6275−6279.
(34) Alexandrescu, A. T.; Snyder, D. R.; Abildgaard, F. *Protein Sci.* **2001**, *10*, 1856−1868.
(35) Banci, L.; Felli, I. C.; Kummerle, R. *Biochemistry* **2002**, *41*, 2913−2920.
(36) Snyder, J. P. *J. Am. Chem. Soc.* **1984**, *106*, 2393−2400.

the solution-state NMR data, from which the population of conformations featuring a γ-turn was estimated to be in the range of 15−30%.

Bearing in mind that Mierke et al. found the βII′-turn to be stable and present in all five conformers, it is safe to assume that at least one of the structures of pA_4 possesses a βII′γ conformation.[10] In a later publication, Nikiforovich and co-workers stated that structures of CPPs "derived directly from NMR data may not correspond to the energy minimum (minima) with low relative conformational energy".[11] In this article, the authors noted that the predominant conformation of pA_4 would not be of the βII′γ-type, and a different set of structural families obtained using independent energy calculations was presented. While these structures fulfill the NOE restraints, they cannot explain the results obtained in the present work.

All structures published by Nikiforovich and co-workers could in principle account for a correlation $Ala3H^N-Ala5C'$ in long-range HNCO experiments, since the amide moiety of Ala3 and the carbonyl group of Ala5 point to the same side of the molecule. In contrast, the amide moiety of Ala5 and the carbonyl group of Ala3 point to *opposite* sides, and thus cannot explain the correlation $Ala3C'-Ala5H^N$ observed in the present work. In addition, none of the structures reported by Nikiforovich et al. matches the REDOR distances (see table S2 in the Supporting Information). Deviations of up to 25% greatly exceed the error margin of the REDOR experiments and indicate that the structures presented by Nikiforovich and co-workers cannot explain our experimental data. Furthermore, all of the structures presented in this work are in accord with the relative positioning of the CαH and NC′ bond vectors and fulfill the "$\phi = -120°$ rule", whereas many of the pA_4 structures proposed by Nikiforovich et al. violate these energetically favored features. All in all, it can be stated that the structures obtained by independent energy calculations are at variance with the NMR and MD data obtained in the present work and therefore do not satisfyingly represent the conformations sampled by pA_4.

In summary, we have reinvestigated the structure of *cyclo*-(−D-Pro−Ala_4−) using solution- and solid-state NMR methods coupled with extensive, fully solvated MD simulations. These detailed, experimental and theoretical data, are in complete accord with the conclusions of an earlier publication by us that pA_4 adopts a conformation with a stable βII′-turn with the D-amino acid in the $i + 1$ position, while the lower half of the molecule around Ala4 is flexible, with transitions between a γ-turn and a conformation with both amides projecting on the same face.[10]

Acknowledgment. The authors thank J. Klages for recording a series of HNCO experiments on γ-pA_4. M.H. acknowledges a Feodor−Lynen fellowship from the Alexander-von-Humboldt Foundation. We thank the Deutsche Forschungsgemeinschaft and the Fonds der Chemischen Industrie for financial support.

Note Added after ASAP Publication. The presentations of DL_4 and LDLL were incorrect in the version published October 3, 2006; the corrected version was published October 11, 2006.

Supporting Information Available: Table of dihedral angles of various pA_4 structures; table of N-C′ distances of various pA_4 structures. This material is available free of charge via the Internet at http://pubs.acs.org.

JA063174A